Solid-State Structures of Base-Free Ytterbocenes and Inclusion Compounds of Bis(pentamethylcyclopentadienyl)ytterbium with Neutral Carboranes and Toluene: The Role of Intermolecular Contacts

Madeleine Schultz, Carol J. Burns, David J. Schwartz, and Richard A. Andersen*,[1]

Chemistry Department and Chemical Sciences Division of Lawrence Berkeley National Laboratory, University of California, Berkeley, California 94720

Received October 18, 1999

The base-free ytterbocenes $(Me_5C_5)_2Yb$, $(Me_4C_5H)_2Yb$, and $[1,3\text{-}(Me_3C)_2C_5H_3]_2Yb$ have been prepared from their diethyl ether adducts, synthesized by reaction of YbI_2 and the sodium salt of the substituted cyclopentadiene anion in diethyl ether. The structures of the base-free molecules have been determined by X-ray crystallography. The molecule $(Me_5C_5)_2Yb$ has been found to crystallize in two different morphologies; the complex also forms inclusion complexes with toluene, *ortho*-carborane, *meta*-carborane, and 1,2-dimethyl-*ortho*-carborane. The ytterbocene molecule in all of the derivatives examined is bent in the solid state with centroid−metal−centroid angles ranging from 132° to 147°. A detailed examination of the structures and comparison with the reported structures of $(Me_5C_5)_2Eu$, $(Me_5C_5)_2Sm$, $[1,3\text{-}(Me_3Si)_2C_5H_3]_2Yb$, and $[1,3\text{-}(Me_3Si)_2C_5H_3]_2Eu$ reveal that bending is the general structural preference. Close inter- or intramolecular contacts are observed in every case between the ytterbium atom and one or more carbon atoms other than those of the two cyclopentadienide rings of that ytterbocene fragment. The packing geometry is dictated by the substituents on the cyclopentadienide rings, the molecules arranging so as to minimize crowding in the solid state. The net result is a coordination polymer, dimer, or monomer, depending on the ring substituents.

Introduction

The solid-state crystal structure of $(C_5H_5)_2Yb$ has been determined recently,[2] thirty-five years after the first report of its synthesis.[3] The only other reported crystal structure of a base-free ytterbocene is that of $[1,3\text{-}(Me_3Si)_2C_5H_3]_2Yb$.[4] Both metallocenes form polymeric chain structures, but the intimate structural details are different. In $(C_5H_5)_2Yb$, the metallocene unit is a bent sandwich with a centroid−Yb−centroid angle of 118°. A cyclopentadienide ring from an adjacent $(C_5H_5)_2Yb$ unit approaches the open side of the wedge, forming a one-dimensional chain structure. The chains are linked together by interchain Yb···H−C interactions with the terminal cyclopentadienide ligands. The one-dimensional microstructure is reminiscent of that of $(C_5H_5)_2Mn$,[5] and the overall structure is similar to that of $(C_5H_5)_2Ca$.[6] The structural similarity between the alkaline earth and divalent lanthanide metallocenes supports the hypothesis that molecules derived from these metals with similar ionic radii have similar solid-state structures for identical ligand sets.[7] Bis(pentamethylcyclopentadienyl)calcium has also been structurally characterized, and it, too, exists as a bent metallocene with a centroid−metal−centroid angle of 147°.[8] In this case, intermolecular interactions result in a linear coordination polymer, discussed in more detail below.

In the solid-state structure of $[1,3\text{-}(Me_3Si)_2C_5H_3]_2Yb$, the metallocene unit is also bent, with a centroid−Yb−centroid angle of 138°.[4] A chain structure of Yb···Me−Si results in a linear coordination polymer. The structure of $[1,3\text{-}(Me_3Si)_2C_5H_3]_2Eu$ is similar.[4] Although the base-free calcium analogue is known, no structural details are available.[9] However, the similarity in sublimation temperatures is not inconsistent with a similar structure. The only other base-free divalent lanthanide metallocenes that have been characterized crystallographically are $(Me_5C_5)_2Eu$ and $(Me_5C_5)_2Sm$.[10] These compounds exist as isostructural bent sandwich structures in the solid state and will be described in greater

(1) Address correspondence to the Chemistry Department, University of California, Berkeley, CA 94720; raandersen@lbl.gov.
(2) Apostolidis, C.; Deacon, G. B.; Dornberger, E.; Edelmann, F. T.; Kanellakopulos, B.; MacKinnon, P.; Stalke, D. *J. Chem. Soc., Chem. Commun.* **1997**, 1047.
(3) Fischer, E. O.; Fischer, H. *Angew. Chem., Int. Ed. Engl.* **1964**, *3*, 132.
(4) Hitchcock, P. B.; Howard, J. A. K.; Lappert, M. F.; Prashar, S. *J. Organomet. Chem.* **1992**, *437*, 177.
(5) Bünder, W.; Weiss, E. *Z. Naturforsch.* **1978**, *13b*, 1235.
(6) Zerger, R.; Stucky, G. *J. Organomet. Chem.* **1974**, *80*, 7.
(7) Shannon, R. D. *Acta Crystallogr., Sect. A* **1976**, *A32*, 751.
(8) Williams, R. A.; Hanusa, T. P.; Huffman, J. C. *Organometallics* **1990**, *9*, 1128.
(9) Engelhardt, L. M.; Junk, P. C.; Raston, C. L.; White, A. H. *J. Chem. Soc., Chem. Commun.* **1988**, 1500.
(10) Evans, W. J.; Hughes, L. A.; Hanusa, T. P. *Organometallics* **1986**, *5*, 1285.

10.1021/om990821g CCC: $19.00
Publication on Web 01/21/2000

detail below as they complement the discussion of the structures of $(Me_5C_5)_2Yb$.

To date the only published structural data for $(Me_5C_5)_2Yb$ is from gas-phase electron diffraction studies.[11−13] In the gas phase, all intermolecular interactions are minimized and $(Me_5C_5)_2Yb$ is monomeric. The thermal average structure is a bent sandwich in which the centroid−Yb−centroid angle is 158°. Bis(pentamethylcyclopentadienyl)calcium is structurally similar in the gas phase, with a centroid−Ca−centroid angle of 154°.[13]

Thus, divalent lanthanide and alkaline earth metallocenes appear to prefer bent sandwich structures in both the gas and condensed phases. Several models have been advanced to rationalize this geometrical preference, including a molecular orbital model,[14,15] an electrostatic (polarized-ion) model,[15,16] and a model based on van der Waals attractive forces.[17,18] To date no single explanation has been accepted. The molecular orbital model is, perhaps, unappealing, as the extent of mixing of the metal valence electrons with ligand orbitals is small for f-block metals. Indeed, it has been explicitly stated that the molecular orbital model cannot account for the bending, as the calculated energy difference between the D_{5d} and C_{2v} structures is too small.[14] However, the 4f-electrons are more polarizable for divalent than for trivalent metals, and some polarization of metal electrons by the ligands is expected for divalent metallocenes. On the other hand, the electrostatic model treats the metal−ligand bonds as purely ionic, and this model does not allow mixing of metal and ligand electrons. Thus, the molecular orbital model overemphasizes covalent mixing, while the electrostatic model underemphasizes it. It can be seen that in those cases in which some polarization occurs, such as for divalent lanthanide metallocenes, these two models are not widely disparate.

Bending a two-coordinate ML_2 molecule results in repulsion as the ligands approach each other at distances closer than the sum of their van der Waals radii. Such repulsion limits the bend angle. The repulsion is related to the metal radius, as a larger metal allows more bending before the ligands approach each other too closely. Generally, Me···Me distances on the order of 4.0 Å are viewed as repulsive since the van der Waals radius of a methyl group is about 2.0 Å. The closest Me···Me inter-ring distance in the gas-phase structure of $(Me_5C_5)_2Yb$ is 4.15 Å, a distance at which the interaction may be stabilizing.[19] This is the origin of the van der Waals model.[13] In choosing among the various models, it is important to remember that the stabilization energy on bending is extremely small, probably on the order of 1−5 kcal/mol,[14,15] and no experiment to date has been able to prove any of the models.

In this paper we provide the synthetic and solid-state X-ray structural details for base-free $(Me_5C_5)_2Yb$, as well as two less completely substituted metallocenes, $(Me_4C_5H)_2Yb$ and $[1,3\text{-}(Me_3C)_2C_5H_3]_2Yb$. In addition, we describe the changes that occur in the solid-state structures of $(Me_5C_5)_2Yb$ when this metallocene is crystallized in the presence of toluene and some neutral carboranes. These inert molecules are nevertheless capable of perturbing the solid-state packing of the metallocene. All of these X-ray studies confirm that the $(Me_5C_5)_2Yb$ fragment, in a variety of lattice environments, is bent.

Results and Discussion

Synthesis and Physical Properties of Base-Free Ytterbocenes. The diethyl ether complex $(Me_5C_5)_2Yb(OEt_2)$ was described previously.[20,21] The other two diethyl ether complexes were prepared similarly, by the reaction of 2 equiv of the sodium salt of the substituted cyclopentadienide with YbI_2 in diethyl ether, followed by filtration and crystallization from the mother liquor (eq 1).[22] Synthetic details and characterization of these diamagnetic adducts are included in the Experimental Section. Base-free $(Me_5C_5)_2Yb$ was prepared by the

$$2NaCp' + YbI_2 \xrightarrow{OEt_2} Cp'_2Yb(OEt_2) + 2NaI \quad (1)$$
$$(Cp' = Me_5C_5,\ Me_4C_5H,\ 1,3\text{-}(Me_3C)_2C_5H_3)$$

toluene reflux method which has previously been used to desolvate the alkaline earth metallocenes,[23] with one key difference: the toluene solution must be refluxing vigorously before the system is exposed to dynamic vacuum (eq 2). If this precaution is not followed, a

$$Cp'_2Yb(OEt_2) \xrightarrow[\text{reflux, vac}]{PhMe} Cp'_2Yb\ (2) \quad (2)$$
$$(Cp' = Me_5C_5,\ 1,3\text{-}(Me_3C)_2C_5H_3)$$

mixture of the base-free compound and the diethyl ether adduct is obtained. This is presumably because $(Me_5C_5)_2Yb$ binds the Lewis base diethyl ether more strongly than do the alkaline earth metallocenes. Sublimation of the etherate does not remove the coordinated diethyl ether; instead, the etherate sublimes intact. The THF complex $(Me_5C_5)_2Yb(thf)$ cannot be desolvated by either the toluene reflux method or sublimation.[24] This contrasts with the complex $[1,3\text{-}(Me_3Si)_2C_5H_3]_2Yb(OEt_2)$, which can be desolvated by sublimation.[4] The adduct $[1,3\text{-}(Me_3C)_2C_5H_3]_2Yb(OEt_2)$ can be desolvated in a manner similar to that used to prepare $(Me_5C_5)_2Yb$. Both of these base-free ytterbocenes are soluble in pentane and can be crystallized from that solvent at low temperature.

(11) Andersen, R. A.; Boncella, J. M.; Burns, C. J.; Blom, R.; Haaland, A.; Volden, H. V. *J. Organomet. Chem.* **1986**, *312*, C49.
(12) Andersen, R. A.; Boncella, J. M.; Burns, C. J.; Green, J. C.; Hohl, D.; Rösch, N. *J. Chem. Soc., Chem. Commun.* **1986**, 405.
(13) Andersen, R. A.; Blom, R.; Boncella, J. M.; Burns, C. J.; Volden, H. V. *Acta Chem. Scand. A* **1987**, *A41*, 24.
(14) Green, J. C.; Hohl, D.; Rösch, N. *Organometallics* **1987**, *6*, 712.
(15) DeKock, R. L.; Peterson, M. A.; Timmer, L. K.; Baerends, E. J.; Vernooijs, P. *Polyhedron* **1990**, *9*, 1919.
(16) Guido, M.; Gigli, G. *J. Chem. Phys.* **1976**, *65*, 1397.
(17) Timofeeva, T. V.; Lii, J.-H.; Allinger, N. L. *J. Am. Chem. Soc.* **1995**, *117*, 7452.
(18) Hollis, T. K.; Burdett, J. K.; Bosnich, B. *Organometallics* **1993**, *12*, 3385.
(19) Pauling, L. *The Nature of the Chemical Bond*; Cornell University Press: Ithaca, NY, 1960.
(20) Tilley, T. D.; Boncella, J. M.; Berg, D. J.; Burns, C. J.; Andersen, R. A. *Inorg. Synth.* **1990**, *27*, 146.
(21) Watson, P. L. Structure of $(Me_5C_5)_2Yb(OEt_2)$, personal communication, 1981.
(22) Khvostov, A. V.; Sizov, A. I.; Bulychev, B. M.; Knjazhanski, S. Y.; Belsky, V. K. *J. Organomet. Chem.* **1998**, *559*, 97.
(23) Burns, C. J.; Andersen, R. A. *J. Organomet. Chem.* **1987**, *325*, 31.
(24) Tilley, T. D.; Andersen, R. A.; Spencer, B.; Ruben, H.; Zalkin, A.; Templeton, D. H. *Inorg. Chem.* **1980**, *19*, 2999.

Table 1. Physical Properties of Base-Free Ytterbocenes

compound	melting point (°C)	color	calculated density (g/cm^3)	reference
$(Me_5C_5)_2Yb$	189−191	brown-black	1.56	this work
$(Me_4C_5H)_2Yb$	324−326	pale green	1.71	this work
$[1,3\text{-}(Me_3C)_2C_5H_3]_2Yb$	85−86	green-brown	1.40	this work
$[1,3\text{-}(Me_3Si)_2C_5H_3]_2Yb$	119−121	purple	1.34	4
$(C_5H_5)_2Yb$	>400	red	2.38	2

Table 2. Unit Cell Parameters for $(Me_5C_5)_2Yb$(black), $(Me_5C_5)_2Yb$(brown), $(Me_5C_5)_2Eu$, and $(Me_5C_5)_2Sm$

compound	*a* (Å)	*b* (Å)	*c* (Å)	*β* (deg)	reference
$(Me_5C_5)_2Yb$(black)	31.013(3)	12.466(2)	9.836(1)	95.960(9)	this work
$(Me_5C_5)_2Yb$(brown)	9.8	12.4	14.9	95	this work
$(Me_5C_5)_2Eu$	9.838(4)	13.443(4)	14.174(3)	95.03(2)	10
$(Me_5C_5)_2Sm$	9.815(3)	13.436(9)	14.163(8)	94.98(4)	10

Bis(tetramethylcyclopentadienyl)ytterbium is fundamentally different from the other substituted ytterbocenes. The dark green etherate $(Me_4C_5H)_2Yb(OEt_2)$ is insoluble in pentane, while the etherates of the other ytterbocenes are soluble in that solvent. Dissolution of $(Me_4C_5H)_2Yb(OEt_2)$ in toluene and slow crystallization at −40 °C gives the base-free molecule. This is in stark contrast to the other ytterbocenes, which cannot be freed of coordinated diethyl ether by crystallization from any hydrocarbon solvent. The base-free $(Me_4C_5H)_2Yb$ can also be prepared by sublimation of the etherate. This also contrasts with $(Me_5C_5)_2Yb(OEt_2)$, which retains diethyl ether upon sublimation. The THF adduct $(Me_4C_5H)_2Yb(thf)_2$ is only sparingly soluble in toluene and diethyl ether and does not sublime.[25] Base-free $(Me_4C_5H)_2Yb$ is completely insoluble in noncoordinating solvents including boiling toluene, while the other substituted base-free ytterbocenes are very soluble in solvents such as pentane. The base-free ytterbocenes sublime under dynamic vacuum. Some of their physical properties are listed in Table 1.

Structures of Base-Free Ytterbocenes. Crystalline $(Me_5C_5)_2Yb$ is obtained in two structural modifications that depend on how it is crystallized. Crystallization from a pentane solution at low temperature gives brown-black needles, $(Me_5C_5)_2Yb$(black). However, if the crystals are heated under reduced pressure, brown-green needles form on the walls of the flask, $(Me_5C_5)_2Yb$(brown). The unit cell parameters for the two crystalline modifications, determined from single-crystal diffraction data, are shown in Table 2, as well as the corresponding data for $(Me_5C_5)_2Eu$ and $(Me_5C_5)_2Sm$. All four of these molecules crystallize in the space group $P2_1/n$. It can be seen that the unit cell of $(Me_5C_5)_2Yb$(black) is an alternate setting of a lattice similar to that of $(Me_5C_5)_2Yb$(brown) but with one cell dimension doubled. Although the two modifications of $(Me_5C_5)_2Yb$ have different cell dimensions and colors, their infrared spectra, as Nujol mulls in the solid state, are superimposable. They have identical melting points and NMR spectra in C_6D_6 solution. Hence, the two forms differ only in how they pack in the solid state.

The brown-green form is presumably isostructural with $(Me_5C_5)_2Eu$ and $(Me_5C_5)_2Sm$ since the unit cell dimensions are similar and their space groups are identical (Table 2). For this reason, the full crystal structure of $(Me_5C_5)_2Yb$(brown) was not determined.

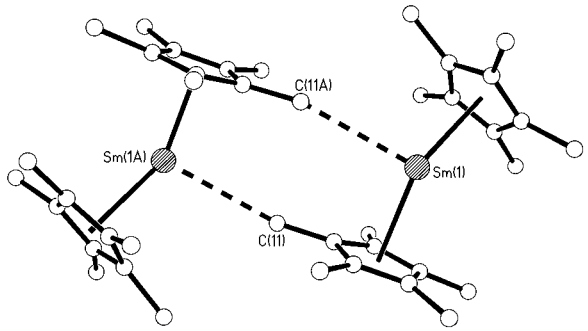

Figure 1. Ball and stick diagram of $(Me_5C_5)_2Sm$ constructed from published coordinates.

Figure 1 shows a ball-and-stick diagram that was constructed from the published coordinates of $(Me_5C_5)_2Sm$. The view shown is different from the published one and is reproduced here since it emphasizes structural features that are helpful in discussing the solid-state structure of $(Me_5C_5)_2Yb$(black). The structures of $(Me_5C_5)_2Eu$ and $(Me_5C_5)_2Sm$ are nearly identical. Each is a bent sandwich metallocene with a centroid−metal−centroid angle of 140°, an average M−C(ring) distance of 2.79(1) Å, and a M−centroid distance of 2.53 Å. In addition, each molecule has one close intermolecular M···C (methyl) distance, 3.22(1) Å for Eu and 3.19(1) Å for Sm. This intermolecular contact involves a methyl group of a molecule related by a crystallographic inversion center and has the net effect of creating a coordination dimer. These discrete dimeric units comprise the solid lattice (Figure 1). Somewhat surprisingly, the methyl group C(11) involved in the intermolecular contact is not the most sterically accessible since it is located at the side of the wedge, not the front.

The room-temperature crystal and diffraction data for the brown-black form of $(Me_5C_5)_2Yb$ are given in Table 3. There are two unique molecules in the asymmetric unit. The important bond lengths and angles are shown in Table 4. The molecular structure of this form is clearly different from that of $(Me_5C_5)_2Eu$ and $(Me_5C_5)_2Sm$ and presumably $(Me_5C_5)_2Yb$(brown). The view in Figure 2 shows that the molecules form a one-dimensional coordination rather than an ensemble of dimeric units. The individual $(Me_5C_5)_2Yb$ fragments are bent sandwiches, with centroid−metal−centroid angles of 146° and 145°. The mean Yb−C(ring) distances in each molecule are 2.66 and 2.67 Å, while the Yb−centroid distance is 2.38 Å for both molecules. The Yb−C(ring) distances are 0.13 Å shorter than the corresponding distances found in $(Me_5C_5)_2Eu$ and $(Me_5C_5)_2Sm$, which

(25) Schumann, H.; Glanz, M.; Hemling, H.; Hahn, F. E. *Z. Anorg. Allg. Chem.* **1995**, *621*, 341.

Table 3. Selected Crystal Data and Data Collection Parameters for $(Me_5C_5)_2Yb$(black), $(Me_4C_5H)_2Yb$, and $[1,3\text{-}(Me_3C)_2C_5H_3]_2Yb$

formula	$C_{20}H_{30}Yb$	$C_{18}H_{26}Yb$	$C_{26}H_{42}Yb$
fw	443.50	415.44	527.66
space group	$P2_1/n$	$P2_12_12_1$	$P2_12_12_1$
a (Å)	31.013(3)	9.9528(3)	11.9795(6)
b (Å)	12.466(2)	10.1141(4)	13.3629(7)
c (Å)	9.836(1)	16.0538(3)	15.5938(8)
β (deg)	95.960(9)	90	90
V (Å^3)	3782(2)	1616.03(7)	2496.3(2)
Z	4	4	4
d_{calc} (g/cm^3)	1.56	1.71	1.40
μ(Mo Kα)$_{calc}$ (cm^{-1})	49.25	57.73	37.54
size (mm)	0.60 × 0.44 × 0.32	0.15 × 0.08 × 0.04	0.14 × 0.09 × 0.05
temp (K)	298	165	145
diffractometer[a]	Enraf-Nonius CAD4	Siemens SMART	Siemens SMART
scan type, range	ω, $3° \le 2\theta \le 45°$	ω, $4° \le 2\theta \le 52°$	ω, $4° \le 2\theta \le 52°$
no. of reflns collected	5577	7842	11 966
no. of unique reflns	4933	1727	4448
no. of obsd reflns	4190	1136	2323
no. of variables	380	172	234
abs corr	Ψ scan	empirical	empirical
transmission range	0.563−1.00	0.825−0.956	0.714−0.928
R^b	0.0206	0.026	0.039
R_w	0.0289	0.024	0.044
R_{all}	0.0379	0.031	0.05
GOF	1.491	0.74	1.29
max. Δ/σ in final cycle	0.11	0	0.02

[a] Radiation: graphite monochromated Mo Kα ($\lambda = 0.71073$ Å). [b] $R = \sum||F_o| - |F_c||/\sum|F_o|$.

Table 4. Selected Bond Lengths (Å) and Angles (deg) for $(Me_5C_5)_2Yb$(black), $(Me_4C_5H)_2Yb$, and $[1,3\text{-}(Me_3C)_2C_5H_3]_2Yb$

	$(Me_5C_5)_2Yb$(black)[a]	$(Me_4C_5H)_2Yb$	$[1,3\text{-}(Me_3C)_2C_5H_3]_2Yb$
Yb−C (ring) (mean) (Å)	2.66; 2.67	2.69	2.66
Yb−C (ring) (range) (Å)	2.636(3)−2.690(3)	2.60(1)−2.733(9)	2.628(9)−2.70(1)
Yb−Cp (centroid) (Å)	2.38; 2.38	2.41	2.37
Cp−Yb−Cp (deg)	146; 145	132	147
twist angle (deg)	21; 25	31	19
backside distance (Å)	3.49; 3.68	3.68	3.87
nonbonded distances (Å)	2.944(4); 3.078(4)	2.81(1)	3.09(1), 3.20(2)

[a] Data for two unique molecules in the asymmetric unit presented as Yb(1); Yb(2).

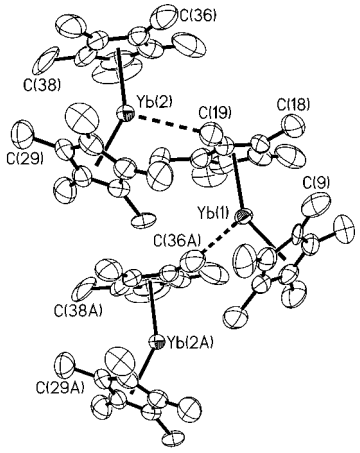

Figure 2. ORTEP diagram of $(Me_5C_5)_2Yb$(black) (50% probability ellipsoids). Hydrogen atoms are omitted for clarity. All non-hydrogen atoms were refined anisotropically, while hydrogen atoms were included in calculated positions.

is expected from a difference of 0.15 Å between the ionic radii of Eu(II) and Yb(II) in six-coordinate environments.[7]

The individual $(Me_5C_5)_2Yb$ molecules are not related by an inversion center; instead, one unit (Yb(1)) twists with respect to the other (Yb(2)), so that Yb(1) forms a close contact with a Me_5C_5 ring in an adjacent asymmetric unit. The close contact distance Yb(1)···C(36A) is 2.944(4) Å, with a methyl group on a Me_5C_5 ring bound to the Yb(2) in an asymmetric unit related by a unit translation along the *c*-axis. The contact is from the side of the metallocene wedge. The Yb(2) has a close contact with a methyl group on a ring bound to Yb(1), with a Yb(2)···C(19) distance of 3.078(4) Å. Again, the C(19) atom is at the side of the metallocene wedge. The net result of these Yb···C contact distances is the linear coordination polymer shown in Figure 2. This is similar to the solid-state structure of $(Me_5C_5)_2Ca$, which also forms a coordination polymer; in that case the intermolecular contact distances Ca···C (methyl) are 2.98 and 3.07 Å for the two unique molecules in the asymmetric unit.[8] The unit cell parameters of $(Me_5C_5)_2Ca$ are very similar to those of $(Me_5C_5)_2Yb$(black), and the molecules crystallize in the same space group. Given the similar ionic radii of calcium and ytterbium, it is not surprising that their decamethylmetallocenes have similar structures.

The strength of the intermolecular interactions (in both forms of $(Me_5C_5)_2Yb$ as well as the calcium, samarium, and europium analogues) is obviously weak; it must be on the order of solvation energies, since the compounds are hydrocarbon soluble. Presumably, the larger metal radii of Sm and Eu result in the less crowded dimeric form, while Yb can adopt either crystalline form.

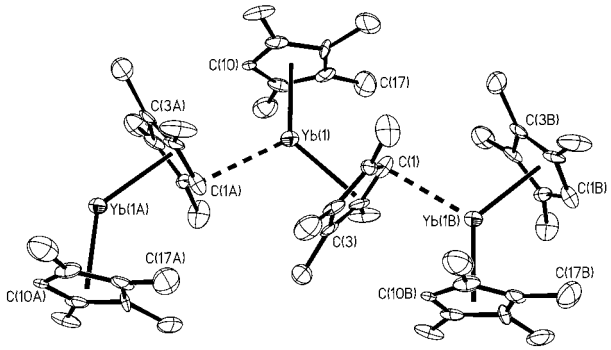

Figure 3. ORTEP diagram of $(Me_4C_5H)_2Yb$ (50% probability ellipsoids). Hydrogen atoms are omitted for clarity. All non-hydrogen atoms were refined anisotropically, while hydrogen atoms were included in calculated positions except for H(1) bound to C(1), which was located in the difference map.

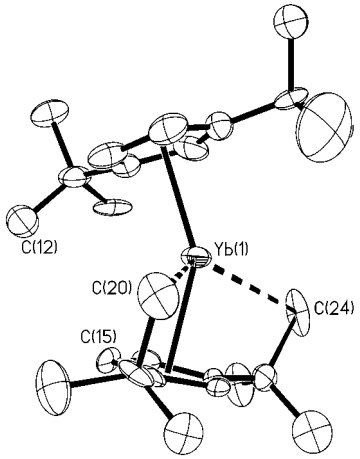

Figure 4. ORTEP diagram of $[1,3\text{-}(Me_3C)_2C_5H_3]_2Yb$ (50% probability ellipsoids). Hydrogen atoms are omitted for clarity. All non-hydrogen atoms were refined anisotropically, except for C(1) and C(17), which were refined isotropically, while hydrogen atoms were included in calculated positions.

Replacing a methyl group with a hydrogen atom on the cyclopentadienide ring does not seem to be a major modification, yet the physical properties of $(Me_5C_5)_2Yb$ and $(Me_4C_5H)_2Yb$ are dramatically different. In particular, the low solubility of $(Me_4C_5H)_2Yb$ resembles that of $(C_5H_5)_2Yb$ rather than $(Me_5C_5)_2Yb$. The solid-state crystal and molecular structure of $(Me_4C_5H)_2Yb$, shown in Figure 3, indicates that the metallocene is a bent sandwich polymer. Crystal data for $(Me_4C_5H)_2Yb$ are shown in Table 3, while selected bond distances and angles are presented in Table 4. The individual $(Me_4C_5H)_2Yb$ units are bent, with a centroid−metal−centroid angle of 132°, which is 13° more bent than the corresponding angle in $(Me_5C_5)_2Yb$(black). The average Yb−C(ring) distance of 2.69 Å and the Yb−centroid distance of 2.41 Å in $(Me_4C_5H)_2Yb$ are about 0.03 Å longer than the equivalent values found in $(Me_5C_5)_2Yb$(black). The range in Yb−C(ring) distances is much greater in $(Me_4C_5H)_2Yb$, 2.60(1)−2.733(9) Å compared with 2.636(3)−2.690(3) Å in $(Me_5C_5)_2Yb$(black). These differences result from the fact that the compound is polymeric, with one ring forming a μ-η^5,η^1-Me_4C_5H bridge.

The bridging ring (C(1)−C(5)) connects the Yb atoms in the polymer chain. All Yb−C distances are equal (2.72(2) Å) in this ring. The shortest intermolecular ytterbium−carbon distance in the molecule (2.81(1) Å) involves the methine atom C(1) of this ring. The hydrogen atom H(1) bound to C(1) was located as the largest peak in the difference map but was not refined. This atom is bent out of the ring plane by 0.21 Å toward the Yb(1) atom of the molecule, away from the Yb(1B) atom involved in the close intermolecular contact. The Yb(1B)···H(1) distance is 3.04 Å, and the Yb(1B)···C(1)−H(1) angle is 91°. This distortion seems to be the result of the Yb(1B) atom seeking the negative electron density at the methine site while pushing the H(1) atom out of the plane of the growing chain in a form of incipient rehybridization. The Yb(1B)···C(1) distance of 2.81(1) Å is 0.13 Å smaller than any intermolecular contact distance in the case of $(Me_5C_5)_2Yb$(black) and is only 0.08 Å longer than the longest intramolecular Yb−C(ring) distance in the structure of $(Me_4C_5H)_2Yb$. Hence, the ytterbium atom can be thought of as bis-η^5,η^1-coordinated, and this is presumably the reason for the low solubility of this ytterbocene.

The terminal ring (C(10)−C(14)) is nearly planar but is not symmetrically bound to the ytterbium atom, having two short Yb−C distances (Yb−C(10), 2.60(1) Å, and Yb−C(14), 2.62(1) Å) and three longer ones (Yb−C(11), 2.67(1) Å, Yb−C(13), 2.70(1) Å, and Yb−C(12), 2.71(1) Å). Atom C(10) is the methine carbon atom of that ring and participates in an intermolecular contact of 3.36(1) Å with C(3), a quaternary carbon atom on the bridging ring of an adjacent molecule.

From a structural perspective, $[1,3\text{-}(Me_3C)_2C_5H_3]_2Yb$ is the simplest ytterbocene yet prepared, Figure 4. Details of the data collection and structure solution and refinement are in Table 3. As indicated in Table 4, it is a bent metallocene with a centroid−metal−centroid angle of 147°, an average Yb−C(ring) distance of 2.66 Å, and an average Yb−centroid distance of 2.37 Å. There is no intermolecular Yb···C contact distance less than 4.0 Å, and this ytterbocene is monomeric in the solid state. There are, however, two short intramolecular Yb···C contact distances of 3.09(1) and 3.20(2) Å, to C(24) and C(20), respectively. These are methyl carbon atoms located on two different *tert*-butyl groups on one ring. As these groups are separated by a methine carbon on the ring, they approach the Yb atom from opposite sides of the wedge.

It is informative to compare the solid-state crystal structure of $[1,3\text{-}(Me_3C)_2C_5H_3]_2Yb$ with that of $[1,3\text{-}(Me_3Si)_2C_5H_3]_2Yb$.[4] A reconstructed ball-and-stick diagram of the Me_3Si derivative, derived from the published coordinates, is shown in Figure 5. In this molecule the centroid−metal−centroid angle is 138°, 9° more bent than in the *tert*-butyl case. The Yb−C(ring) and Yb−centroid distances are the same for the two molecules. In $[1,3\text{-}(Me_3Si)_2C_5H_3]_2Yb$, the small centroid−metal−centroid angle allows a close intermolecular contact between a methyl carbon atom C(9) on one metallocene unit and the Yb atom of a neighboring unit of 2.872(7) Å. This results in a coordination polymer similar to the other ytterbocene polymers described above. An intermolecular interaction is presumably prevented in the *tert*-butyl derivative since the centroid−metal−centroid angle cannot be smaller than its value of 147° without

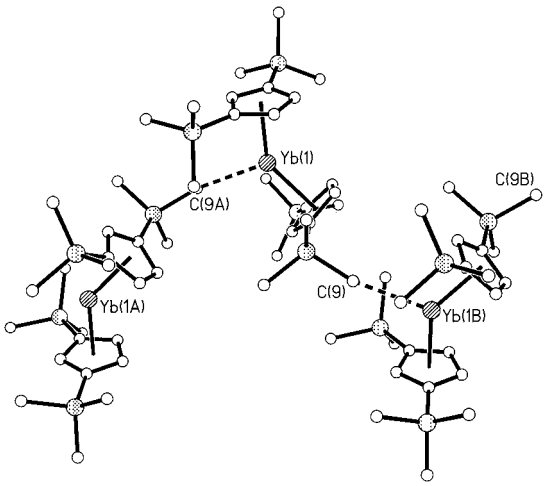

Figure 5. Ball-and-stick diagram of $[1,3\text{-}(Me_3Si)_2C_5H_3]_2$-Yb constructed from published coordinates.

unfavorable backside steric interactions between the *tert*-butyl groups on the rings, so the metal is effectively shielded from adjacent molecules. In the Me_3Si derivative, the rings are nearly staggered (twist angle 33°) and the four Me_3Si groups are symmetrically arranged about the open side of the wedge. This arrangement allows the backside C(ring)···C(ring) contact to be minimized despite the small centroid−metal−centroid angle.

Discussion of Base-Free Ytterbocenes. In the condensed phase, the intermolecular interactions observed for all of the ytterbocenes have the effect of compressing the centroid−metal−centroid angle relative to the gas-phase value found for $(Me_5C_5)_2Yb$ of 158°.[13] The angle in these coordination oligomers is similar to that found in ytterbocene Lewis base adducts.[24,26,27] This suggests that the base-free metallocenes associate to higher aggregates in order to maximize their bonding interactions. In every case there are intramolecular carbon−carbon distances on the backside of the wedge that are less than the sum of the van der Waals radii (4.0 Å) (Table 4).

The overall packing geometry (dimer, polymer, or monomer) is dependent on the substituents on the rings and how the molecules arrange to maximize the bonding interactions and minimize the steric repulsions between various groups.[28] The calculated densities of the molecules give some indication of how efficiently the structures are packed; $(Me_4C_5H)_2Yb$ has a density of 1.71 g/cm^3, which is greater than the densities of the other substituted ytterbocenes (Table 1). The higher calculated density is consistent with the insolubility and very close Yb···C interaction found in $(Me_4C_5H)_2Yb$. The trend in melting points of the ytterbocenes is also consistent with the observed intermolecular interactions; $(Me_4C_5H)_2Yb$ melts above 300 °C, while $[1,3\text{-}(Me_3C)_2C_5H_3]_2Yb$ melts below 100 °C (Table 1).

In the case of $(Me_5C_5)_2Yb$, the energy difference between dimer and polymer is clearly minimal, as either form can be isolated depending on how the molecule is crystallized. This hypothesis is reinforced by the manner in which $(Me_5C_5)_2Yb$ packs into the crystalline lattice when neutral molecules cocrystallize with it, as described below. Inclusion compounds evidence the same type of coordination oligomers of $(Me_5C_5)_2Yb$ units as those just described. In addition, these forms may be readily interconverted thermally, emphasizing the small energy differences involved.

Table 5. Infrared Spectra of Carboranes and Their Inclusion Complexes

compound	ν_{CH} (cm^{-1})	ν_{BH} (cm^{-1})
o-$H_2C_2B_{10}H_{10}$	3070vs	2604vs, 2578vs
$(Me_5C_5)_2Yb$(*o*-$H_2C_2B_{10}H_{10}$)	3074m, 3010vs	2610vs, 2575vs, 2563s
m-$H_2C_2B_{10}H_{10}$	3064s	2603vs
$(Me_5C_5)_2Yb$(*m*-$H_2C_2B_{10}H_{10}$)	3066w, 3024vs	2601vs
o-$Me_2C_2B_{10}H_{10}$		2586vs
$(Me_5C_5)_2Yb$(*o*-$Me_2C_2B_{10}H_{10}$)		2591vs

Inclusion Compounds with $(Me_5C_5)_2Yb$. The sterically and electronically unsaturated ytterbium center in $(Me_5C_5)_2Yb$ is expected to coordinate any molecule with a permanent dipole moment, and many examples of such coordination involving small molecules have been described.[24,26,27] These are classic Lewis acid−base complexes. However, a large polar molecule that does not fit in the wedge cannot coordinate in that manner, and the question arises as to whether a weak interaction over a long distance could be observed. To explore this question, the reactions of $(Me_5C_5)_2Yb$ with the polar molecules *ortho*-, *meta*-, and 1,2-dimethyl-*ortho*-carborane were investigated.

The dipole moment of *ortho*-carborane is 4.31 D, the carbon atoms being located at the positive end of the dipole.[29,30] *Meta*-carborane has a lower dipole of 2.78 D, while the dipole of 1,2-dimethyl-*ortho*-carborane is thought to be somewhat lower than that of *ortho*-carborane. When *ortho*-carborane and $(Me_5C_5)_2Yb$ are mixed in hexane, an immediate precipitation of a green solid is observed. The solid can be recrystallized from hot toluene to give dark green needles in good yield. The analogous complexes with *meta*-carborane and 1,2-dimethyl-*ortho*-carborane are somewhat more soluble, but both can be crystallized from hexane at −25 °C. Analytical data reveal that the complexes all have a carborane:Yb ratio of 1:1. The room-temperature solution ^{1}H NMR spectra of the adducts (in C_6D_6) are unchanged from the spectra of their constituent molecules. The IR spectra show lowered C−H stretching frequencies for the carboranes in the adducts compared with the free carboranes, while the B−H stretching frequencies are unchanged (Table 5). This suggests that $(Me_5C_5)_2Yb$ is perturbing the carborane C−H bonds. This is unexpected, as that is the positive end of the carborane dipole.

These $(Me_5C_5)_2Yb$(carborane) complexes are green when isolated at low temperature. When the 1,2-dimethyl-*ortho*-carborane complex is allowed to warm to room temperature, it is found to consist of two crystalline forms: one that remains green at all temperatures, and one that turns orange above 5 °C. This color change is reversible. The *meta*-carborane complex remains green to 95 °C, at which temperature it reversibly turns orange. The *ortho*-carborane complex

(26) Burns, C. J.; Andersen, R. A. *J. Am. Chem. Soc.* **1987**, *109*, 915.
(27) Burns, C. J.; Andersen, R. A. *J. Am. Chem. Soc.* **1987**, *109*, 941.
(28) Hays, M. L.; Hanusa, T. P. *Adv. Organomet. Chem.* **1997**, *40*, 117.
(29) Laubengayer, A. W.; Rysz, W. R. *Inorg. Chem.* **1965**, *4*, 1513.
(30) Maruca, R.; Schroeder, H.; Laubengayer, A. W. *Inorg. Chem.* **1967**, *6*, 572.

Table 6. Selected Crystal Data and Data Collection Parameters for $(Me_5C_5)_2Yb(o\text{-}H_2C_2B_{10}H_{10})$, $(Me_5C_5)_2Yb(o\text{-}Me_2C_2B_{10}H_{10})$, and $(Me_5C_5)_2Yb$(toluene)

formula	$C_{22}H_{42}B_{10}Yb$	$C_{24}H_{46}B_{10}Yb$	$C_{27}H_{38}Yb$
fw	587.73	615.78	535.64
space group	$P2_1/c$	$P2_1/c$	$P\bar{1}$
a (Å)	12.780(1)	13.061(1)	10.086(6)
b (Å)	10.047(1)	10.822(1)	10.510(6)
c (Å)	21.175(3)	21.814(2)	11.813(6)
α (deg)	90	90	76.31(4)
β (deg)	91.18(1)	93.211(9)	87.63(5)
γ (deg)	90	90	80.69(6)
V (Å^3)	2718.3(8)	3079(1)	1200.5(17)
Z	4	4	2
d_{calc} (g/cm^3)	1.47	1.33	1.482
μ(Mo Kα)$_{calc}$ (cm^{-1})	34.39	57.73	38.9
size (mm)	0.27 × 0.16 × 0.12	0.28 × 0.27 × 0.26	0.27 × 0.16 × 0.12
temp (K)	298	298	161
diffractometer[a]	Enraf-Nonius CAD4	Enraf-Nonius CAD4	Enraf-Nonius CAD4
scan type, range	$\theta-2\theta$, $2\theta \le 45°$	$\theta-2\theta$, $2\theta \le 45°$	$\theta-2\theta$, $2\theta \le 45°$
no. of reflns collected	3988	4502	3364
no. of unique reflns	3543	4016	3054
no. of reflns, $F_o^2 > 3\sigma(F_o^2)$	2117	3072	2489
no. of variables	299	317	253
abs corr	analytical	analytical	DIFABS
transmission range	0.624−0.685	0.471−0.594	0.67−1.00
R[b]	0.0196	0.026	0.036
R_w	0.0239	0.0329	0.0448
R_{all}	0.102	0.0647	0.036
GOF	1.486	1.516	2.128
max. Δ/σ in final cycle	0.01	0.01	0

[a] Radiation: graphite monochromated Mo−Kα ($\lambda = 0.71073$ Å) [b] $R = \Sigma||F_o| - |F_c||/\Sigma|F_o|$

Table 7. Selected Bond Lengths (Å) and Angles (deg) for $(Me_5C_5)_2Yb(o\text{-}H_2C_2B_{10}H_{10})$, $(Me_5C_5)_2Yb(o\text{-}Me_2C_2B_{10}H_{10})$, and $(Me_5C_5)_2Yb$(toluene)

	$(Me_5C_5)_2Yb(o\text{-}H_2C_2B_{10}H_{10})$	$(Me_5C_5)_2Yb(o\text{-}Me_2C_2B_{10}H_{10})$	$(Me_5C_5)_2Yb$(toluene)
Yb−C(ring) (mean) (Å)	2.67	2.63	2.67
Yb−C(ring) (range) (Å)	2.647(5)−2.685(4)	2.619(5)−2.651(4)	2.645(8)−2.702(8)
Yb−Cp (centroid) (Å)	2.38	2.35	2.38
Cp−Yb−Cp (deg)	143	147	142
twist angle (deg)	28	35	30
backside distance (Å)	3.50	3.79	3.53
nonbonded distances (Å)	3.076(5), 3.284(5)	2.987(5)	2.966(9), 3.10(1)

is green at all temperatures. This thermochroism is reminiscent of that of $(Me_5C_5)_2Yb$ itself, which reversibly turns orange at 130 °C.

The crystal structures of the green *ortho*-carborane complex and the 1,2-dimethyl-*ortho*-carborane complex in its orange form were determined at 25 °C in order to elucidate the details of the metal−carborane interaction. The crystal data for the structures are listed in Table 6, while selected bond distances and angles are given in Table 7. The results are unexpected as it is apparent that the ytterbocene and the carborane molecules are entirely noninteracting (Figures 6, 7). The $(Me_5C_5)_2Yb$ fragment has a close intermolecular contact with itself in each structure and forms a dimer or polymer with overall geometries reminiscent of the base-free $(Me_5C_5)_2$-Yb structures (brown and black) just described.

In the crystal structure of the *ortho*-carborane complex (Figure 6), the centroid−metal−centroid angle is 143° and two close carbon−ytterbium intermolecular contact distances are observed; the Yb···C(26) distance is 3.076(5) Å, and the Yb···C(20) distance is 3.284(5) Å. Atom C(26) is at the open edge of the wedge and interacts with the ytterbium atom of an adjacent $(Me_5C_5)_2Yb$ unit, while atom C(20) (which is at the side of the wedge and on the other ring) interacts with a different $(Me_5C_5)_2Yb$ unit. The net effect is to create a coordination polymer, similar to that found for $(Me_5C_5)_2$-Yb(black).

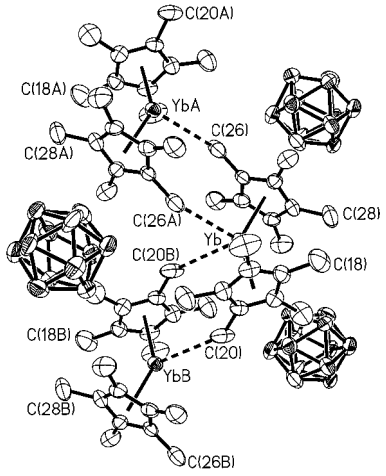

Figure 6. ORTEP diagram of $(Me_5C_5)_2Yb(o\text{-}H_2C_2B_{10}H_{10})$ (50% probability ellipsoids). Hydrogen atoms are omitted for clarity. All non-hydrogen atoms were refined anisotropically, while hydrogen atoms were included in calculated positions.

The centroid−metal−centroid angle in the 1,2-dimethyl-*ortho*-carborane complex is 147°, and the intermolecular contact occurs between Yb and C(26) with a distance of 2.987(5) Å. As in the cases of $(Me_5C_5)_2Eu$ and $(Me_5C_5)_2Sm$, this contact is with a molecule related by a crystallographic inversion center and has the result

Table 8. Unit Cells of $(Me_5C_5)_2Yb(o\text{-}H_2C_2B_{10}H_{10})$ at 25 °C and $(Me_5C_5)_2Yb(o\text{-}Me_2C_2B_{10}H_{10})$ at −80 and at 25 °C

	$(Me_5C_5)_2Yb(o\text{-}H_2C_2B_{10}H_{10})$	$(Me_5C_5)_2Yb(o\text{-}Me_2C_2B_{10}H_{10})$	$(Me_5C_5)_2Yb(o\text{-}Me_2C_2B_{10}H_{10})$
temp (K)	298	193	298
color	dark green	green	orange
a (Å)	12.780(1)	13.109(1)	13.061(1)
b (Å)	10.047(1)	10.655(2)	10.822(1)
c (Å)	21.175(3)	21.117(4)	21.814(2)
β (deg)	91.18(1)	93.04(1)	93.211(9)

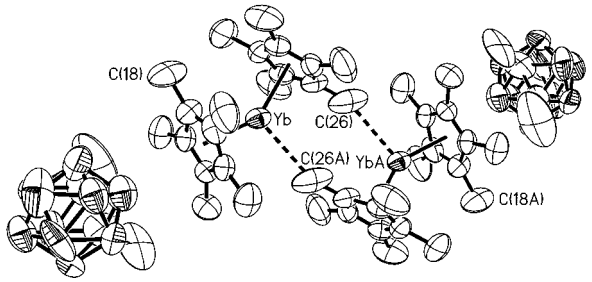

Figure 7. ORTEP diagram of $(Me_5C_5)_2Yb(o\text{-}Me_2C_2B_{10}H_{10})$ (50% probability ellipsoids). Hydrogen atoms are omitted for clarity. All non-hydrogen atoms were refined anisotropically, while hydrogen atoms were included in calculated positions except for the carborane methyl hydrogen atoms, which were not placed.

of creating the coordination dimer shown in Figure 7. Thus, the net structure of the $(Me_5C_5)_2Yb$ portion of this inclusion compound is very similar to that suggested for base-free $(Me_5C_5)_2Yb$(brown).

The coordination polymer chains in the structure of the *ortho*-carborane complex are parallel to the *b*-axis, and the *b*-axis of the 1,2-dimethyl-*ortho*-carborane complex is longer, presumably because the chains are broken up into dimeric units. In an attempt to discern whether the thermochroism observed in the 1,2-dimethyl-*ortho*-carborane complex is due to a structural phase change, the unit cell of the green form of the thermochroic 1,2-dimethyl-*ortho*-carborane complex was determined at −80 °C (unfortunately the crystals were damaged, and a complete structure could not be determined) (Table 8). At that temperature the *b*-axis is shorter, which supports the idea that the polymeric green form converts to the dimeric orange form at higher temperature. The longer *b* dimension is due to the dimeric units occupying more space than the more efficiently packed polymer.

The molecule $(Me_5C_5)_2Yb$ can also form solvates. Crystallization of $(Me_5C_5)_2Yb$ from a toluene/pentane mixture yields a compound that is a 1:1 $(Me_5C_5)_2Yb$/toluene adduct by elemental analysis and ^1H NMR spectroscopy. The ^1H NMR chemical shifts in C_6D_6 are unchanged from the values of the constituent molecules. The solid-state X-ray structure was determined; crystal data are given in Table 6, bond distances and angles are presented in Table 7, and an ORTEP diagram is shown in Figure 8. Again, the metallocene units and solvent molecules are entirely noninteracting in the solid state. The $(Me_5C_5)_2Yb$ units form a coordination polymer that is essentially identical to the $(Me_5C_5)_2Yb$ fragment of the *ortho*-carborane complex and to $(Me_5C_5)_2$-Yb(black). The centroid−metal−centroid angle of the toluene complex is 142°, and there are two close intermolecular contact distances: Yb···C(19) 2.966(9) Å and Yb···C(6) 3.10(1) Å. The C(6) and C(19) are both on the sides of the wedge, and the close contacts are with different $(Me_5C_5)_2Yb$ units, resulting in a polymer.

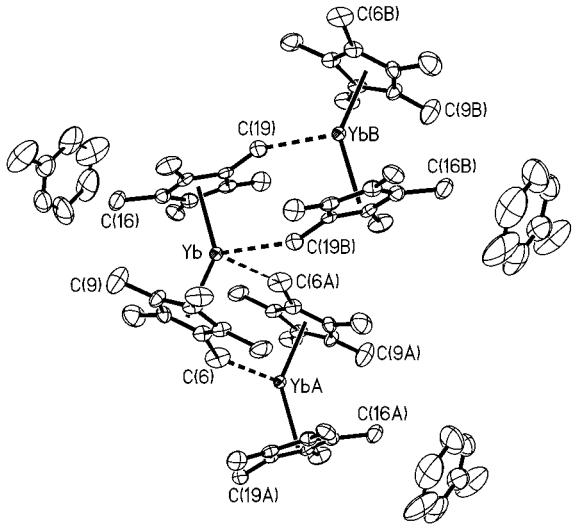

Figure 8. ORTEP diagram of $(Me_5C_5)_2Yb$(toluene) (50% probability ellipsoids). Hydrogen atoms are omitted for clarity. All non-hydrogen atoms were refined anisotropically, while hydrogen atoms were included in calculated positions.

Discussion of Inclusion Complexes. The inclusion complexes illustrate that the intermolecular interactions of the ytterbocene are more important than the lattice energy that would be obtained by coordination of toluene or a carborane. The structures of the $(Me_5C_5)_2Yb$ fragments in the clathrates are almost identical to those in the pure molecule. Comparison of the structures of the *ortho*-carborane complex and the 1,2-dimethyl-*ortho*-carborane complex shows that the energy difference between the dimeric and polymeric forms is minimal. The solubility of the clathrates is lower than that of the base-free ytterbocene, presumably because the lattice energy is somewhat greater.

The structure of base-free $(Me_5C_5)_2Yb$ and the structures that are formed when that molecule cocrystallizes with these large neutral molecules differ in subtle ways. The base-free metallocene crystallizes in two forms, one a dimer, likely to be identical to the structure of $(Me_5C_5)_2Eu$ and $(Me_5C_5)_2Sm$. The other form is a polymeric relative of the dimer in which the rings are reoriented slightly so that there is one more intermolecular contact than in the dimer. This is presumably the result of an increase in enthalpy in the crystalline system overcoming the loss in entropy. The inclusion compounds allow the $(Me_5C_5)_2Yb$ fragment to form dimeric and polymeric motifs, with the more disordered phase being favored at higher temperature. Thus, all of the slight structural changes in the complexes described here can be understood as a subtle balance between ΔH and $T\Delta S$.

Epilogue. The solid-state X-ray crystallographic studies of the ytterbocenes presented here show that their natural geometry is bent. The extent of bending

is determined by the number and size of the substituents on the cyclopentadienide rings. The solid-state packing can be influenced by cocrystallizing $(Me_5C_5)_2Yb$ with neutral molecules, but the bent geometry of the metallocene is a constant feature. The cause of bending is most reasonably traced to the ionic nature of the cyclopentadienide−ytterbium(II) bond, moderated by some polarization. For a molecule ML_2, the bent geometry is lower in energy than the linear one,[16] and in the case of organometallic derivatives, van der Waals attractive forces supplement the natural bent geometry.

Experimental Details

General Comments. All reactions and product manipulations were carried out under dry nitrogen using standard Schlenk and drybox techniques. Dry, oxygen-free solvents were employed throughout. The elemental analyses and mass spectra were performed at the analytical facility at the University of California at Berkeley. The following compounds were prepared as previously described: Me_5C_5H,[31] $NaNH_2$,[32] YbI_2,[20] Me_5C_5Na,[33] $(Me_5C_5)_2Yb(OEt_2)$,[20] 1,3-$(Me_3C)_2C_5H_4$,[34] and $Me_4C_5H_2$.[35] Me_4C_5HNa and [1,3-$(Me_3C)_2C_5H_3$]Na were prepared by procedures analogous to that used to synthesize Me_5C_5Na.[33]

$(Me_4C_5H)_2Yb(OEt_2)$. A procedure identical to that used to prepare $(Me_5C_5)_2Yb(OEt_2)$ was employed,[20] and the product was isolated in 53% yield. Under dynamic vacuum, the complex loses the coordinated diethyl ether at 80 °C. ^{1}H NMR (C_6D_6): δ 5.65 (s, 2H), 2.98 (q, 4H, J = 7 Hz), 2.21 (s, 12H), 2.03 (s, 12H), 0.93 (t, 6H, J = 7 Hz) ppm.

[1,3-$(Me_3C)_2C_5H_3]_2Yb(OEt_2)$. A procedure similar to that used to prepare $(Me_5C_5)_2Yb(OEt_2)$ was employed,[20] with the difference that the slurry did not become green immediately upon addition of solvent. Stirring at 25 °C for 15 min resulted in a green slurry; this was then stirred overnight. The isolated yield of green crystals was 78%. Under dynamic vacuum, the complex loses the coordinated diethyl ether at 65 °C. Anal. Calcd for $C_{30}H_{52}OYb$: C 59.9, H 8.71. Found: C 59.9, H 8.94. ^{1}H NMR (C_6D_6): δ 6.06 (d, 4H, J = 2.6 Hz), 5.66 (t, 2H, J = 2.5 Hz), 3.29 (q, 4H, J = 6 Hz), 1.32 (s, 36H), 1.01 (t, 6H, J = 6 Hz) ppm.[22]

$(Me_5C_5)_2Yb$. The ether complex $(Me_5C_5)_2Yb(OEt_2)$ (3.0 g, 5.8 mmol) was dissolved in a minimum of toluene (160 mL), and the green solution was transferred to a long-necked 250 mL round-bottomed flask equipped with a greaseless J.Young tap and containing a magnetic stir bar. The flask was opened to dynamic vacuum briefly, closed, and then heated to 100 °C. The solvent was removed under dynamic vacuum over a period of 2 h, the black residue was redissolved in toluene (160 mL), and the procedure was repeated. The residue was then extracted into pentane (200 mL) and filtered into a large Schlenk tube. The volume of solvent was then reduced to 120 mL under dynamic vacuum, and upon cooling the solution to −40 °C green crystals were formed that became tan upon exposure to vacuum: yield, 1.0 g, 40%. The compound reversibly turns orange-red at 130 °C and melts at 189−191 °C. Anal. Calcd for $C_{20}H_{30}Yb$: C 54.2, H 6.82. Found: C 53.8, H 6.96. NMR spectra (C_6D_6, 20 °C), ^{1}H: δ 1.92 (s) ppm. ^{13}C{^{1}H}: δ 113.4, 10.61 ppm. Mass spectrum m/z = 444 (M^+).

[1,3-$(Me_3C)_2C_5H_3]_2Yb$. A procedure identical to that used to prepare $(Me_5C_5)_2Yb$ was followed. The isolated yield was 60%, mp 85−86 °C. Anal. Calcd for $C_{26}H_{42}Yb$: C 59.2, H 8.02. Found: C 58.5, H 8.24. ^{1}H NMR (C_6D_6, 20 °C) δ 5.95 (d, 4H, J = 2.8 Hz), 5.62 (t, 2H, J = 2.7 Hz), 1.29 (s, 36H) ppm.

$(Me_4C_5H)_2Yb$. The etherate $(Me_4C_5H)_2Yb(OEt_2)$ (0.9 g, 1.8 mmol) was dissolved in toluene (80 mL). The volume of solvent was reduced to 50 mL, and the green solution was cooled to −40 °C. The pale green crystals of the base-free metallocene were isolated in 65% yield (0.5 g), mp 324−326 °C. Anal. Calcd for $C_{18}H_{26}Yb$: C 52.0, H 6.31. Found: C 51.3, H 5.58. The compound does not color toluene at reflux; its insolubility in noncoordinating solvents prevented recrystallization or the measurement of an NMR spectrum.

$(Me_5C_5)_2Yb(o\text{-}H_2C_2B_{10}H_{10})$. $(Me_5C_5)_2Yb$ (0.26 g, 0.59 mmol) was dissolved in hexane (20 mL) and added with stirring to a slurry of *ortho*-carborane (0.080 g, 0.55 mmol) in hexane (5 mL). A green precipitate formed as the *ortho*-carborane dissolved. The solution was allowed to stir for 10 h, and the green precipitate was collected by filtration. The yield of green solid was 0.28 g (87%), mp 205−207 °C. The solid could be recrystallized from a minimum volume of hot toluene to give dark green needles. Anal. Calcd for $C_{22}H_{42}B_{10}Yb$: C 45.0, H 7.22. Found: C 44.1, H 7.38. ^{1}H NMR (C_6D_6, 20 °C): δ 1.91 (s, 30H), 1.74 (s, $\nu_{1/2}$ = 12 Hz, 2H) ppm. ^{1}H NMR of *ortho*-carborane (C_6D_6, 20 °C): δ 2.11 (s, $\nu_{1/2}$ = 16 Hz) ppm.

$(Me_5C_5)_2Yb(o\text{-}Me_2C_2B_{10}H_{10})$. $(Me_5C_5)_2Yb$ (0.28 g, 0.63 mmol) was dissolved in hexane (20 mL) and added with stirring to a solution of 1,2-dimethyl-*ortho*-carborane (0.11 g, 0.64 mmol) in hexane (10 mL); no color change was observed. The solution was filtered, the volume of the filtrate was reduced to 10 mL, and the solution was cooled to −25 °C. The first batch of product was isolated as green crystals, which reversibly turned orange above +5 °C. The second crop of crystals was of two kinds: the thermochroic form and green crystals, which stayed green at room temperature. The two kinds of crystals were identical spectroscopically. The combined yield was 77%; mp 170−172 °C (orange); 195−197 °C (green). Anal. Calcd for $C_{24}H_{46}B_{10}Yb$: C 46.8, H 7.54. Found: C 47.0, H 7.71. ^{1}H NMR (C_6D_6, 20 °C): δ 1.94 (s, 30H), 1.14 (s, 6H) ppm. ^{1}H NMR of 1,2-dimethyl-*ortho*-carborane (C_6D_6, 20 °C): δ 1.17 (s) ppm.

$(Me_5C_5)_2Yb(m\text{-}H_2C_2B_{10}H_{10})$. A procedure analogous to that used to synthesize $(Me_5C_5)_2Yb(o\text{-}Me_2C_2B_{10}H_{10})$ resulted in the formation of green bladelike crystals that turn brown at 60 °C and orange at 95 °C and melted at 186−188 °C (the color changes are reversible). The yield was 69%. Anal. Calcd for $C_{22}H_{42}B_{10}Yb$: C 45.0, H 7.22. Found: C 45.1, H 7.20. ^{1}H NMR (C_6D_6, 20 °C): δ 1.93 (s) (only one peak observed). ^{1}H NMR of *meta*-carborane (C_6D_6, 20 °C): δ 1.97 (s, $\nu_{1/2}$ = 16 Hz) ppm.

Crystallographic Studies. Details of the crystallographic studies are included in the Supporting Information. Selected crystal data and data collection parameters are in Tables 3 and 6, while selected bond lengths and angles are in Tables 4 and 7.

Acknowledgment. This work was partially supported by the Director, Office of Energy Research, Office of Basic Energy Sciences, Chemical Sciences Division of the U.S. Department of Energy, under Contract No. DE-AC03-76SF00098. We thank the Fanny and John Hertz Foundation for a fellowship (C.J.B.), the NSF for a fellowship (D.J.S.), and Dr. Fred Hollander for assistance with the crystallography.

Supporting Information Available: Details of crystallographic studies, further discussion of the structures, atomic positions and anisotropic thermal parameters, tables of bond lengths and angles, and least squares planes for each structure are available. This material is available free of charge via the Internet at http://pubs.acs.org. Structure factor tables are available from the authors.

OM990821G

(31) Manriquez, J. M.; Fagan, P. J.; Schertz, L. D.; Marks, T. J. *Inorg. Synth.* **1982**, *21*, 181.
(32) Greenlee, K. W.; Henne, A. L. *Inorg. Synth.* **1946**, *2*, 128.
(33) Bercaw, J. E.; Marvich, R. H.; Bell, L. G.; Brintzinger, H. H. *J. Am. Chem. Soc.* **1972**, *94*, 1219.
(34) Venier, C. G.; Casserly, E. W. *J. Am. Chem. Soc.* **1990**, *112*, 2808.
(35) Fendrick, C. M.; Schertz, L. D.; Day, V. W.; Marks, T. J. *Organometallics* **1988**, *7*, 1828.